Journal of Constructional Steel Research 103 (2014) 159–167

Contents lists available at ScienceDirect

Journal of Constructional Steel Research

Buckling design of steel tied-arch bridges

Hans De Backer *, Amelie Outtier, Philippe Van Bogaert

Bridge Research Group, Department of Civil Engineering, Ghent University, Technologiepark 904, B-9052 Ghent, Belgium

ARTICLE INFO

Article history:
Received 30 August 2012
Accepted 5 September 2014
Available online 26 September 2014

Keywords:
Steel tied-arch bridge
Buckling
Buckling curves
Design method

ABSTRACT

The structural behaviour of steel tied-arch bridges is determined by the introduction of a large compressive force. As a consequence, slender steel arches are highly sensitive to in-plane as well as out-of-plane buckling. At present, no specific buckling curves for out-of-plane buckling exist for non-linear or curved elements in the international codes and calculation methods. Hence, the buckling curves for straight columns, as determined by ECCS, are used, which leads to considerable inaccuracies in the assessment of the critical buckling load for arch bridges.

This paper presents two practical calculation methods to design for the buckling behaviour of slender steel arch bridges. The first one follows the calculation method of the Eurocode, but proposes some augmented empirical formulas for the buckling length of the arches. This allows for a better representation of the out-of-plane stiffness of the arch cross section and of the wind bracings between both arches.

In addition a second method is proposed, based on the use of simplified finite element models to determine the relative slenderness of the structure. Both methods are validated using results from very detailed three dimensional finite element models. Finite element models of several tied-arch bridges have been created. These models include variations of the bridge length, dimensions of the arch cross-section, boundary condition, and load type. The conclusion of these calculations is that for both of the proposed methods a higher buckling curve can be used than proposed by the code, thus resulting in a more slender bridge design.

1. Introduction

The fundamental behaviour of tied-arches is based on the fact that a large compressive force is developed in the arch cross-section. Because of this, steel arches in particular can become highly sensitive to the out-of-plane buckling phenomenon. However, there is no clear and generally accepted calculation method to predict numerically this stability problem. On one hand, the buckling strength of a steel tied-arch bridge can be calculated by considering the non-linear elastic–plastic behaviour. As the imperfections of the arches highly influence the non-linear behaviour, these geometrical imperfections need to be known before starting this analysis. On the other hand, a linear calculation, resulting in an elastic buckling factor for the compression force, can be carried out. A multiplication factor for the occurring stresses can be found based on this calculation, using an adequate buckling curve, as mentioned for straight beams in [1–3]. In this case as well, the arch imperfections should be known beforehand. However, the imperfections in slender steel arch bridges are not related to those of a straight beam or column which makes it fundamentally impossible, or at least overly safe, to use the standard buckling curves, derived for straight beams.

As the imperfections of arch bridges are smaller than can be expected for straight members, every detail of the bridge becomes important while determining the buckling load and may influence the results of the numerical simulations. Therefore, all details, such as diaphragms, connection plates, orthotropic plated bridge deck, bearing systems and arch springs, are modelled in a very exact manner for the calculations which are the basis of this research paper.

In comparison, most available research has focused on smaller parts of the overall problem, or on simplifications of the situation. Initial studies by Pi and Trahair [4] focussed on the inelastic buckling of arches under uniform compression and uniform bending separately to better understand the background of the buckling behaviour. The actual load situation is however much more complex. A lot of international research has furthermore concentrated on the out-of-plane stability of roller bent steel I-shaped cross-sections [5,6]. These results are certainly relevant but will differ quite a bit in terms of out-of-plane stiffness characteristics and residual stress distributions when compared with the box sections typical for steel arch bridges. Some studies exist focussing on box sections, such as Manzanares Japón and Sánchez-Barbudo [7], but especially the boundary conditions at the supports of the arches are still theoretical constructions. The specific contribution of the research in this paper is thus that it models a realistic situation of an arch with the actual stiffeners, load introductions and boundary conditions. Only the newest research trend in this field [8–10], the influence of temperature gradients on arch buckling, is neglected.

* Corresponding author. Tel.: +32 9 264 54 34; fax: +32 9 264 58 37.
E-mail address: Hans.DeBacker@UGent.be (H. De Backer).

http://dx.doi.org/10.1016/j.jcsr.2014.09.004
0143-974X/

2. Eurocode design of arch buckling

A detailed analytic calculation method has been developed in the Eurocode [1,2], which allows for the determination of the buckling strength of steel members. The first step of this method is the determination of a dimensionless slenderness parameter, λ, for the cross-section of the considered member. Based on this slenderness factor and a correct choice for the buckling curve, a reduction factor, χ, can be directly determined. This clearly defines the maximal normal force in the cross-section before buckling occurs as a reduction of the plastic carrying capacity. While initially developed for straight members, the method is also applicable for curved sections, after some small augmentations.

For arches, the slenderness λ, can be calculated using the following formula:

$$\overline{\lambda} = \sqrt{\frac{A \cdot f_y}{N_{cr}}} \tag{1}$$

where A is the area of the arch cross-section, f_y the yield strength of steel and N_{cr} the critical elastic normal force of the arch. The critical elastic normal force for out-of-plane buckling of steel tied-arch bridges can be determined based on analytical calculations or by simplified finite element modelling using only beam elements for the entire bridge and solving the eigenvalue problem (see Method I in Section 4). An easier method, also supplied by the Eurocode [2] but in an informative Annex D, uses the following formula:

$$N_{cr} = \left(\frac{\pi}{\beta l}\right)^2 EI_z \tag{2}$$

wherein l represents the bridge span, EI_z the out-of-plane bending stiffness of the arch and β the buckling length factor (see also Method II in Section 5). The buckling length factor is the product of two factors β_1 and β_2, which can be found in diagrams in Annex D of Eurocode 3 [2]. The first factor, β_1, is mainly based on the span to height ratio of the arch and the out-of-plane bending stiffness. In addition, the hanger configuration of the arch and the transfer method of loads between arch and bridge deck are represented by β_2.

The reduction factor for the buckling force can afterwards be determined based on the slenderness, using the following formula:

$$\chi = \frac{1}{\Phi + \sqrt{\Phi^2 + \overline{\lambda}^2}}, \chi \leq 1 \tag{3}$$

$$\Phi = 0,5\left(1 + \alpha(\overline{\lambda} - 0,2) + \overline{\lambda}^2\right) \tag{4}$$

where the parameter α determines the choice of the buckling curve and equals 0.34 for buckling curve "b" and 0.21 for buckling curve "a". This factor allows for determining the maximal allowable load on the bridge, or in other words the necessary reduction of the theoretical maximal load capacity because of buckling:

$$N_{b,RD} = \chi \frac{A \cdot f_y}{\gamma_{M1}} \tag{5}$$

where γ_{M1} is a safety factor, determined by Eurocode [1].

3. Finite element modelling of arch buckling

3.1. Description of the FEM geometry

A finite element model of the Albert Canal Bridge, which can be seen in Fig. 1, is used as the basis for the research on the resistance to out-of-plane buckling of arches [11–13]. The detailing and calculation strategy is envisioned to represent the real-life behaviour of an arch bridge during buckling. The Albert Canal Bridge was built in 2004, in Belgium near the city of Antwerp, as part of the new high speed railway between Antwerp and Amsterdam. The bridge span equals 115 m, which is quite larger than the Albert Canal itself. However, this bridge span has been chosen in view of the further widening of the canal and the increasing of fluvial traffic on the canal towards the Port of Antwerp. The two arches of this steel tied-arch bridge are connected to the lower chord members by sixteen inclined hangers. The upper bracing consists of three tubes of large diameters spread along the length of the arch. The arch springs are tied by the lower chord, consisting of an orthotropic steel deck plate. The bridge is furthermore supported by neoprene bearing systems.

To obtain a finite element model which is as accurate as possible, special attention is given to all details of the bridge, as is being described further on, especially those which might introduce asymmetry into the model or might influence the buckling behaviour of the bridge. Since any out-of-plane movement of the bridge is mainly resisted by the wind bracings and by lateral clamping of the arch springs, it was important to model these as accurate as possible. They are the only part of the construction, connecting both bridges and resisting lateral forces.

The model has been developed using the SAMCEF Solver Suite, distributed by LMS Samtech — Siemens [14]. Except for the bearings, the bridge model is constructed of nearly 50,000 Mindlin shell elements. The elements used allow taking into account shear deformations of thick shells. All parts of the arches, the hangers, the connections between the hangers and arches, the diaphragms and the bracings have been modelled in detail.

The finite element model, developed for this bridge can be seen in Fig. 2. Since the lower chord member of this steel tied-arch bridge consists of an orthotropic plated bridge deck, which has a very specific behaviour, the deck plate of the Albert Canal bridge is also modelled in detail, as can be seen in Fig. 3. The longitudinal and transversal stiffness of the orthotropic plated deck are distributing the traffic loads to the lateral lower chord and thus to the arches by means of the hangers. For further clarification of the illustration of the bridge deck in Fig. 3, the deck plate has been removed, displaying the trapezoidal stiffeners

Fig. 1. High-speed railway bridge across the Albert Canal, Antwerp, Belgium.

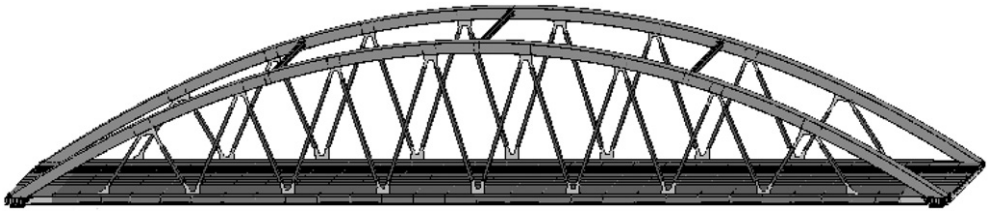

Fig. 2. Finite element model of the Albert Canal Bridge.

and the crossbeams. The lower chord consists of two longitudinal girders with an inverted T-cross-section. These two girders are connected by crossbeams. Furthermore, the deck plate is stiffened by 10 longitudinal closed section stiffeners. These stiffeners cross the crossbeams through special cut-outs in the webs, to avoid a very negative fatigue detail.

At the arch springs, the arch compression forces are introduced in the deck plate. The thickness of the bridge parts and especially the deck plate and crossbeam, is higher, the bridge deck being equipped with additional longitudinal and transversal stiffeners, as can be seen in Fig. 4. Special attention was given to the bearings and the connection between the arch springs and the lower chord edge members. A first calculation run of the model has shown that a torsional effect exists at the arch springs, this fading rapidly with increasing distance to the springs. Torsion is introduced by the neoprene bearings, which are not completely identical for the two arches, resulting in unsymmetrical end conditions. A neoprene bearing system, for which the movement is restrained transversely, can still move about a millimetre in that direction. The same applies to the longitudinally and the fully restrained bearings. This necessitates the use of approximately 2000 volume elements. A flexible/flexible contact between the neoprene and the fixing studs has been assumed. For this, a contact element has been created, with a kinematic constraint that is active when contact occurs and inactive without contact conditions.

Both of the arches of the bridge are stiffened using diaphragms and longitudinal stiffeners, at the connection of the arch with the hangers and at the connection of the arch with the tubular wind bracings. The diaphragms at the connection with the hangers can be seen in Fig. 5. To allow for a better visibility of the diaphragms, one web plate has been removed from the model. In the lower flange plate of the arch, a longitudinal gap is designed, allowing the connection plate with the hangers to enter the arch without connecting it to the lower flange, which would result in extreme local stresses. This connection plate also extends into the hangers, which have a rectangular shape. This plate introduces the hanger forces into the arch. The connection between the arch and the connection plate is made by two diaphragms, which are welded to both ends of the connection plate, which ensures that the hanger forces are transmitted to the arch cross-section as evenly as possible. These diaphragms also increase the resistance of the arch cross-section to distortion.

Other stiffened sections are found at the connection with the tubular wind bracings. The wind bracing tubes are connected to the arch sections, and on both ends of these bracings, diaphragms are installed inside of the arch, as can be seen in Fig. 6. Again, in this figure one web plate of the arch section, as well as the wind bracing itself are removed to deliver a better view on the diaphragms. These two diaphragms are connected to each other by two additional longitudinal stiffeners.

Afterwards, finite element models have been developed for a number of other bridges which have been built in the period of 2004–2008 as part of the high-speed railway network in Belgium: IJzerlaan Bridge, Kapelse Steenweg Bridge, Bredabaan Bridge, Schaarbeek Bridge and Prester Bridge. They incorporate a wide variation in geometries, hanger configurations, wind bracings, etc. The finite element models of the other five considered bridges are quite similar. The arches, stiffeners, bracings and hangers are all built up in a comparable manner. The main difference between these bridges can be found in the deck plates. While the larger bridges are equipped with orthotropic steel deck plates, the smaller ones all have a concrete bridge deck, working together with steel crossbeams and stiffeners. The same level of detail has been used in the development of the finite element models. An overview of the most important dimensions is given in Table 1. In addition, all of the finite element models were parameterized ensuring that the geometry could be varied resulting in more than 50 detailed models of steel tied-arch bridges.

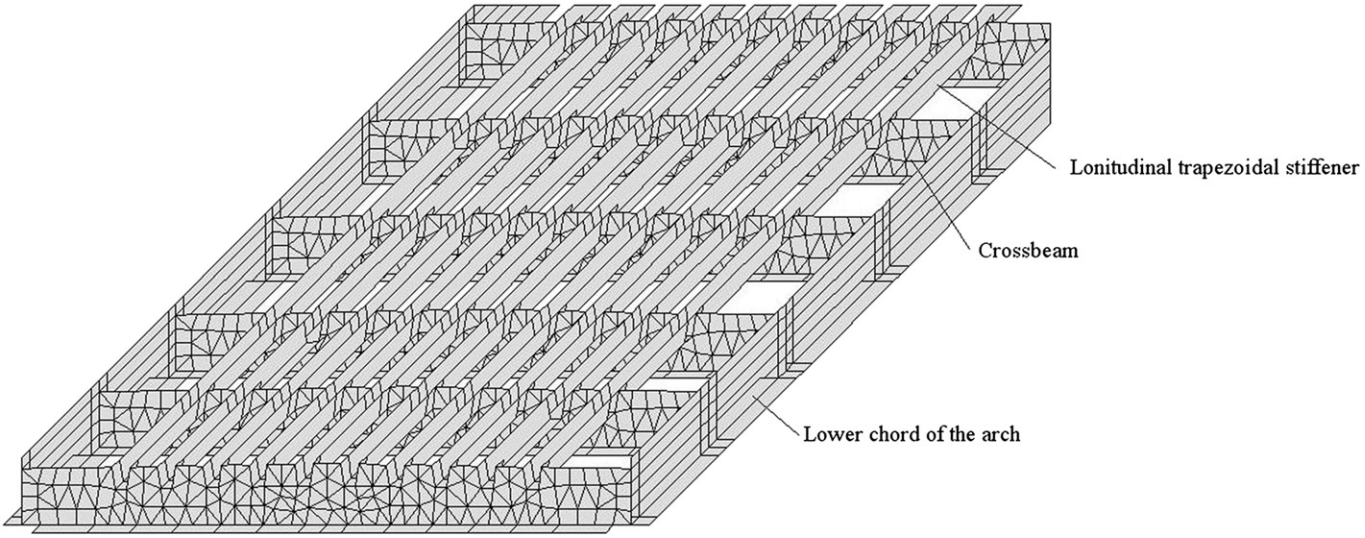

Fig. 3. Detail of the bridge deck in the finite element model of the Albert Canal Bridge.

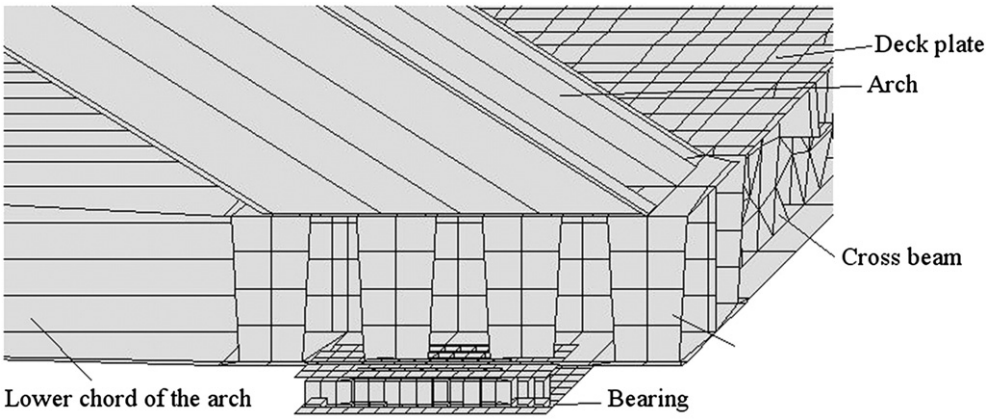

Fig. 4. Detail of the arch springs in the finite element model of the Albert Canal Bridge.

3.2. FEM of buckling

In order to model the buckling behaviour, out-of-plane imperfections have to be introduced before increasing the loading until buckling occurs. This process is illustrated in Fig. 7, showing the transversal out-of-plane displacements of the highest point of the arch of the IJzerlaan Bridge during all steps of the calculation. The possible out-of-plane imperfections are superposed on the actual arch geometry by translating all points of the cross-section in a stress-free manner before the start of the calculations (start of the calculation in Fig. 7). All of the enforced imperfections are based on sine waves with, for the Albert Canal Bridge, maximum amplitude of 115 mm. This amplitude equals 1/1000 fraction of the total the arch span, which is the value recommended by the buckling curves from ECCS [3]. The recommended value according to Eurocode 3 [2] is much higher. Both predictions for the geometrical imperfections are listed in Table 1 for all of the considered bridges. Since concurrent research has proven that the assumed imperfections in design codes are higher than in reality and that a half wine wave is a good approximation of the imperfection shape [15], the geometrical imperfections for steel tied-arch bridges are assumed to be identical to those of straight member according to ECCS [3], being 1/1000th of the arch length. Several possible shapes of out-of-plane imperfections, such as sinusoidal, double sinusoidal and random shapes are then superposed on the model of the bridge, to assess their influence on the buckling behaviour. The imperfections of both arches of each bridge can be identical anti-symmetrical or completely unrelated resulting in another parameterization of the finite element model.

A subsequent calculation is of the elastic–plastic type, using non-linear plastic material behaviour laws for the steel parts of the structure. The definition of this material law complies with Eurocode [1] guidelines for the finite element modelling of plastic materials. The load acting on the bridge is increased linearly and the calculation is stopped, if the displacements of the bridge become as large; any further increase would inevitably result in an infinite increase of displacements. This calculation starts while having the dead load of the structure, which is calculation step “a” in Fig. 7. In the following time steps, the live load consisting of heavy lorries is placed on the bridge deck and is being increased stepwise. Starting from the following time step, the weight of these lorries is increased linearly until the end of the calculation is reached by divergence of the finite element calculation criterion, which is step “f” in Fig. 7. The other steps of the calculation, shown in Fig. 7 are: step “b” which is just before reaching yield strength in the

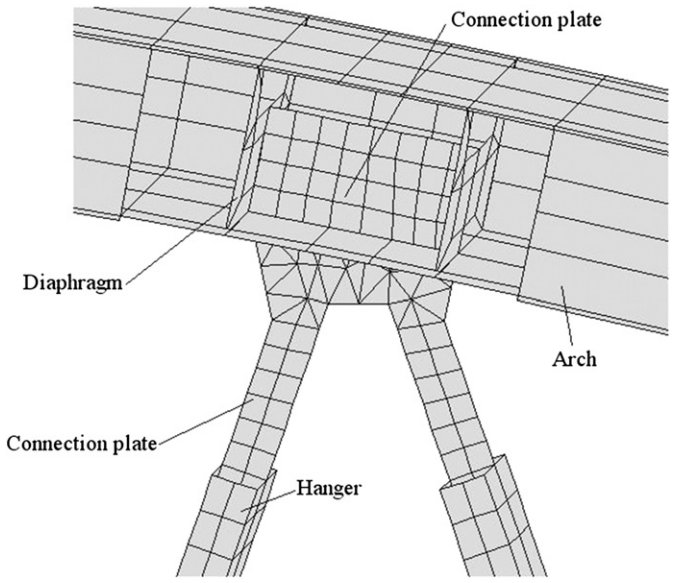

Fig. 5. Detail of the stiffening of the arch cross-section at the connection with hangers in the finite element model of the Albert Canal Bridge.

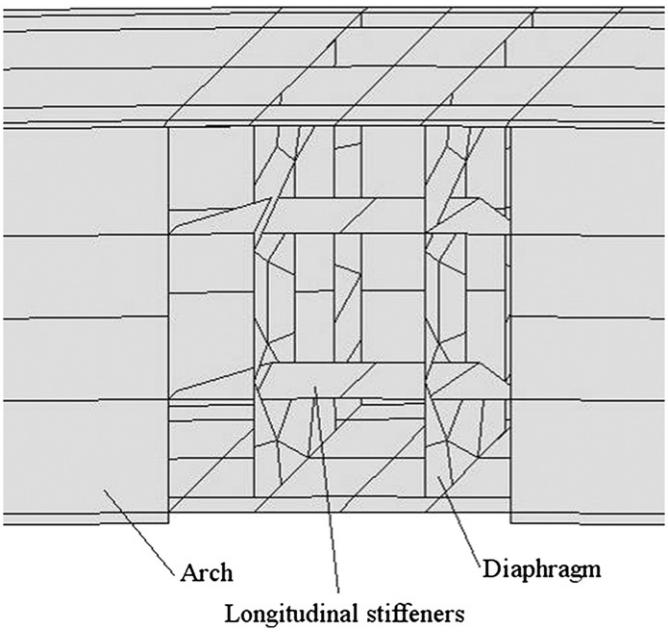

Fig. 6. Detail of the stiffening of the arch cross-section at the connection with wind bracings in the finite element model of the Albert Canal Bridge.

Table 1
Dimensions and load test parameters of the tested bridges.

	Albert Canal Bridge	IJzerlaan Bridge	Kapelse Steenweg Bridge	Bredabaan Bridge	Schaarbeek Bridge	Prester Bridge
Bridge length [m]	115	59	60	60	136.2	136.2
Bridge height [m]	15	9.2	12	12	23.6	23.6
Arch height [mm]	1332	680	686	686	1500	1500
Arch width [mm]	920	850	850	850	1100	1100
Geometrical imperfection according to ECCS [2] [mm]	115	59	60	60	136	136
Geometrical imperfection according to Eurocode [1] [mm]	195	163	139	139	210	210

arch cross-section; step “c” the development of the first plastic hinge near the top of one of both arches of the bridge; the moment “d” where the first plastic hinge is fully formed; expansion of the plastic regions in step “e” and finally step “f” which is characterized by fully formed plastic hinges in both arches after which the bridge structure becomes a mechanism. The buckling reduction factor can be calculated based on the maximum value $N_{FE,pl}$ of the normal force in the finite element model of the arch bridge before buckling of the arch.

$$\chi_{FE} = \frac{N_{FE,pl}}{A \cdot f_y} \tag{6}$$

This non-linear method to determine the buckling factors is chosen over the classic calculation method for buckling, which is based on solving an eigenvalue problem. The difference between both methods is illustrated in Fig. 8 displaying the possible transversal displacements according to a classical buckling calculation (full lines) and the non-linear method proposed here (dashed lines). The advantages of this non-linear method include the possibility to study the internal force distribution during buckling, the fact that displacements of the structure before buckling are taken into account, the actual occurrence of plastic hinges during the calculation, the stabilizing effect both arches can have on each other and the fact that only live load is increased during the calculation while dead load remains constant. Whenever χ_{FE} is used in this paper, it represents a buckling factor based on this type of calculation using plastic behaviour laws, influence of residual stresses, geometrical imperfections, etc. in an extremely detailed finite element model. The calculation method will always be described as the “non-linear method”. To be clear, although the term “non-linear” is used, this calculation is not merely using a non-linear material model or bifurcation theory, but specifically residual stresses, geometrical imperfections, plastic behaviour, etc. In addition, χ_{FE} is assumed to be representative for the actual buckling behaviour and used as a measurement point for all other buckling calculation methods (Eurocode, simplified beam models, etc.).

By modelling several variations of each bridge, it became possible to assemble a database of the actual buckling behaviour of more than 50 steel tied-arch bridges with a span length varying between 45 and 200 m. This database is then used to validate both of the design methods described in the following paragraphs.

4. Buckling design of arch bridges using simplified beam models (Method I)

Using finite element models as detailed as the one in Section 3.1 is not really acceptable for design purposes. Therefore an alternative design method is necessary. Two possible methods, based on the principles of Eurocode 3 [2] design, will be presented in this and the following paragraph.

A simplified finite element model, using only 1-dimensional beam elements can suffice to get an accurate estimation of the buckling strength of an arch bridge. This finite element model does not include the influence of residual weld stresses, nor geometrical imperfections. It is a model of a “perfect” version of the arch bridge upon which a stability analysis can be performed. A stability analysis consists in solving an eigenvalue problem in the form of:

$$Kx = \chi Sx \tag{7}$$

where K represents the structural stiffness matrix, S the geometric stiffness matrix in stability, x one of the buckling modes and χ the associated buckling load. The components of vector x are the structure's degrees of freedom, usually displacements (translations and rotations). The buckling load must be interpreted as the factor by which the external loads must be multiplied for the structure to become unstable. This calculation method is much easier and faster than the one described

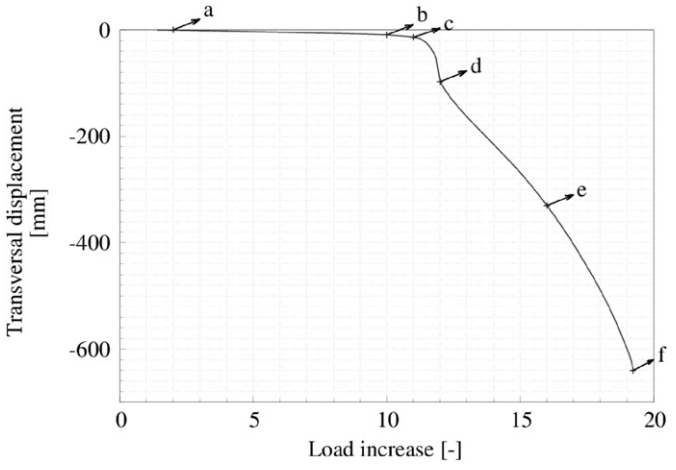

Fig. 7. Transversal displacements of the top of the arch of the IJzerlaan Bridge under increasing live load.

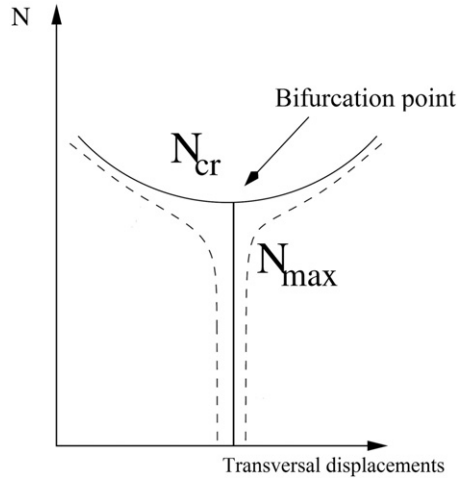

Fig. 8. Comparison between a non-linear buckling calculation and a calculation based on solving the eigenvalue problem.

Table 2
Arch normal force [kN] under dead load and live load as well as the critical normal forces for buckling.

	Albert Canal Bridge	IJzerlaan Bridge	Kapelse Steenweg Bridge	Bredabaan Bridge	Schaarbeek Bridge	Prester Bridge
Dead load	8430	7835	6514	6514	13,540	13,540
Live load	7775	4621	4376	4376	8614	8614
N_{cr} based on a simplified beam model	39,824	53,233	44,085	44,085	103,561	103,561
N_{cr} based on a non-liner model	36,516	51,338	42,772	42,772	91,756	91,756

in previous paragraphs. Table 2 offers a comparison of the critical buckling loads according to this method as well as based on the non-linear method described in Section 4. The difference between both methods is about 10%, with the non-linear method always giving a more conservative value of the buckling force. It is important to remark that the simplified beam-model always uses a "perfect" arch without initial imperfections.

The slenderness λ can thus be calculated using Eq. (8) based on the maximum value $N_{FE,el}$ of the normal force in the finite element model of the arch bridge before buckling of the arch in a calculation using only linear elastic material models. This normal force is illustrated in Fig. 9, showing the simplified version of the finite element model shown in Fig. 2. The most critical buckling mode, also shown in Fig. 10, appears to be a sinusoidal deformation of both arches.

$$\overline{\lambda_{FE}} = \sqrt{\frac{A \cdot f_y}{N_{FE,el}}} \tag{8}$$

When using the slenderness as defined by Eq. (8), it becomes possible to calculate the reduction factor χ for buckling, using Eqs. (3) and (4) based on the results of the simplified beam model. Still, the choice remains whether to use buckling curve "a" or "b" for this calculation step. If the buckling reduction factor, as determined by the non-linear method and Eq. (6) is plotted on the same diagram as the buckling curves, it can be seen that almost all of the arch bridges end up well above buckling curve "a". The slenderness, which is drawn on the horizontal axis, is calculated based on the simplified beam model and Eq. (8) to allow for comparison between χ_{FE} and the buckling curves. Most of points in Fig. 11 are even situated above bucking curve "a_0".

Based on these results, it would seem that buckling curve "a" would be a safe and economical choice for the design of the out-of-plane buckling behaviour of steel tied-arch bridges. However, most codes advise the use of buckling curve "b" at present. It seems advisable to use buckling curve "a" for the design of steel tied-arch bridges, having a welded box section as arch cross-section and with span lengths of about 50 tot 200 m.

5. Buckling design of arch bridges using buckling length factors (Method II)

Fig. 12 shows a comparison of the buckling reduction factor, once determined using buckling curve "b" and the slenderness according to Eq. (2) and once based on the elastic–plastic finite element calculations (non-linear method) described in the previous paragraphs which represents the actual buckling behaviour. It is, in other words a comparison between a method purely using values from Eurocode with a method strictly using the finite element modelling. All of the data points are situated well above the bisector line. It is thus obvious that the calculation using buckling curve "b" and Annex D [2] underestimates the actual buckling capacity of the bridge. In addition, the values for bridges with larger span lengths, longer than 200 m, are situated at the right side of the diagram in Fig. 12. The other bridges, having smaller span lengths are situated further from the bisector line, indicating that the present design codes are even more conservative for shorter spans. It can be postulated that the most important source of the differences between both buckling factors is the definition of the dimensionless slenderness λ, which is determined by the definition of the buckling length factor β.

Using Eq. (2) and the results of the simplified finite element model discussed in Section 4 as well as the non-linear model described in Section 3, it is possible to recalculate the actual values for the buckling length factor β based on the maximum value $N_{FE,el}$ of the normal force in the simplified finite element model. The values according to the tables in Annex D of Eurocode 3 [2] are shown on the horizontal axis of the diagram in Fig. 13. The vertical axis represents the value of the buckling length factor β for the same fifty arch bridges, but calculated based on Eq. (2) and finite element calculations. It seems that the variation of the buckling length factor is in reality much larger than assumed in the Eurocode 3 [2]. In addition, the difference seems especially important for the larger span bridges with heavier cross-sections.

A variation that large indicates that other parameters need to be taken into account in addition to the influencing factors mentioned in Eurocode [2]. At the moment, Eurocode [2] mainly bases the buckling length factor on the ratio between the bridge height and the bridge span, f/l. All of the considered bridges have f/l-ratios varying between 0.16 and 0.19 which gives buckling length factors varying between 0.39 and 0.42 according to Annex D of Eurocode 3 [2] which is a very small variation. In reality, a much larger variation between 0.20 and 0.55 is found, which suggests that a number of other parameters influence the buckling length factor.

Because of this large difference in buckling length factors, an alternative determination formula for the buckling length factor is proposed, usable for bridges with a height to span ratio between 0.15 and 0.20. This alternative method assumes the buckling length factor to be mainly determined by the bridge span, l, as was illustrated in Fig. 13, and also influenced by the bending stiffness of the arch cross-section for out-of-plane bending, I_z. This is illustrated in Fig. 14. Comparable bridges are drawn using the same symbol, indicating that longer bridges are grouped more to the bottom of the diagram. Bridges with the same

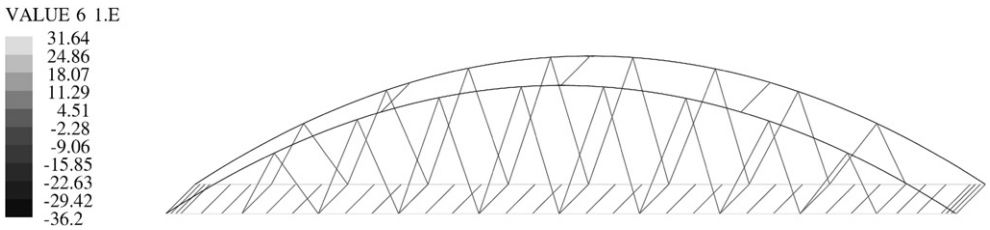

Fig. 9. Normal force [N] in the arch when buckling occurs in a simplified finite element model of the Albert Canal Bridge.

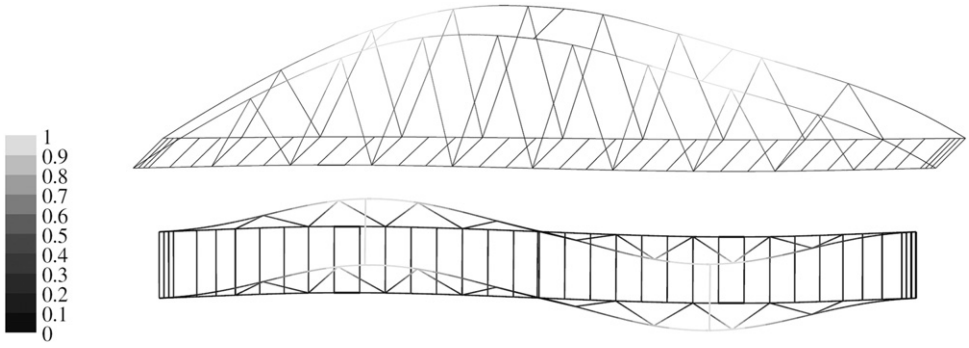

Fig. 10. Buckling shape of the Albert Canal Bridge according to a simplified finite element model.

bridge span apparently show a linear connection between the buckling length factor and I_z. The trend lines for the four groups of data points in Fig. 14 all cross the vertical axis at a value of about 0.255. Still the slope of the four groups of data points is clearly different. The trend line for the largest bridges is almost horizontal, while the smaller bridges clearly have a much steeper variation. This indicates that a relation exists between the span length and the steepness of the trend line through points with comparable out-of-plane stiffness.

Based on these observations, the following formula can be proposed for the determination of the buckling length factor, usable for bridges with a height to span ratio between 0.15 and 0.20:

$$\beta_{alt} = \beta_A + I_z(\beta_B - l\beta_C). \tag{9}$$

Based on the parametric finite element analyses, the coefficients of Eq. (9) are determined to be: $\beta_A = 0.255$; $\beta_B = 16.939$ and $\beta_C = 0.114$. The length, l, is given in metres, while the out-of-plane bending stiffness is in m^4. The buckling length factor for all fifty considered arch bridges as determined using Eq. (9) can be compared with the actual buckling length factor based on detailed non-linear finite element modelling in Fig. 15. When comparing Fig. 15 with Fig. 13 it is immediately obvious that the alternative method for calculating the buckling length factor is a much better representation of the actual buckling behaviour, since all values are situated in a narrow zone close to the bisector line of the diagram.

Using the alternative formula for the buckling length factor it is possible to also calculate an alternative dimensionless slenderness λ, using Eqs. (2) and (1). Afterwards, Eqs. (3) and (4) and the Eurocode 3 [2] assumption that the use of buckling curve "b" is correct will allow for determining an alternative buckling reduction factor $\chi_{alt,b}$. The comparison

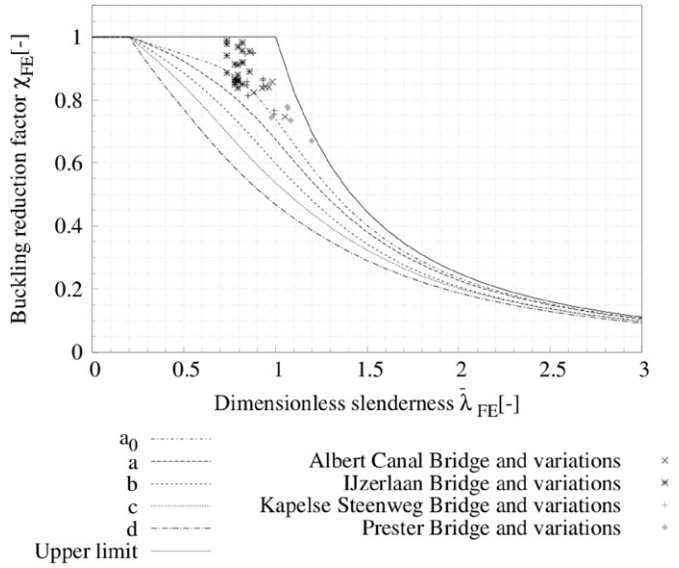

Fig. 11. Comparison of calculation results with a simplified beam model with buckling curves.

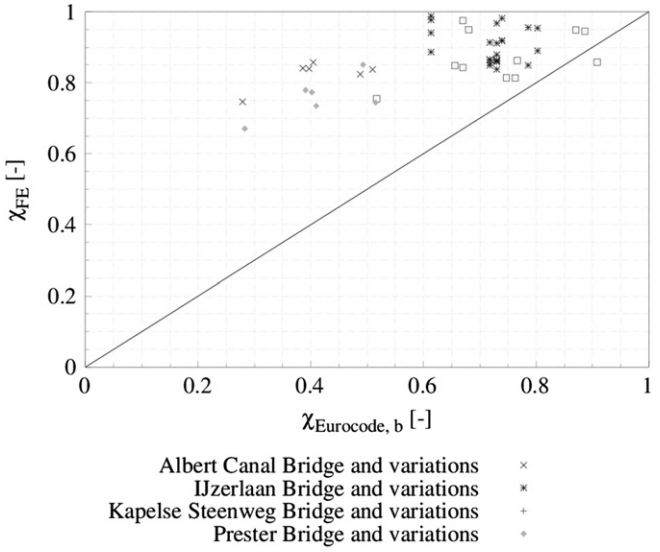

Fig. 12. Comparison of buckling factors based on Eurocode according to buckling curve "b" with results based on detailed non-linear finite element modeling.

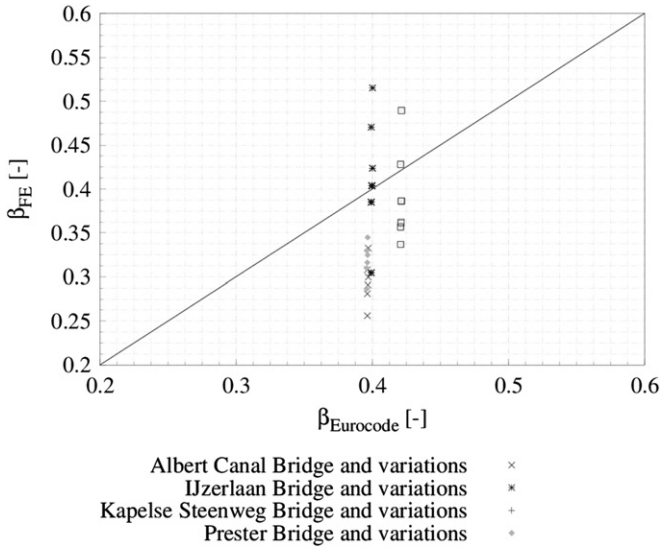

Fig. 13. Comparison of buckling length factors as determined by strict Eurocode and detailed non-linear finite element modeling.

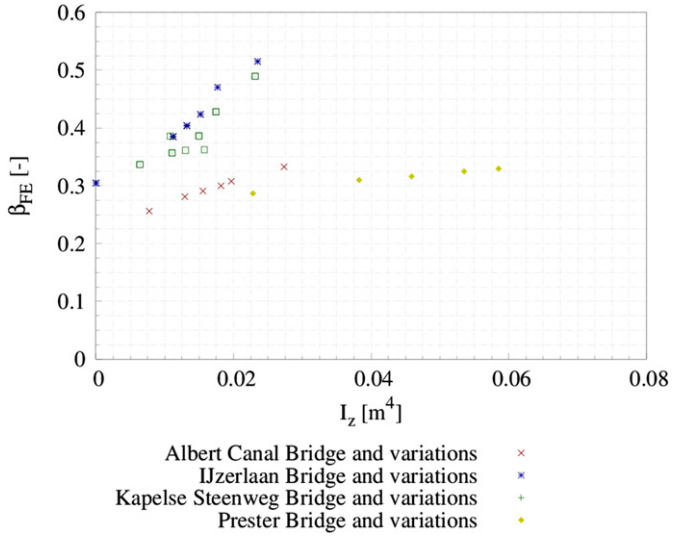

Fig. 14. Relation between buckling length factor and the out-of-plane bending stiffness of the arch cross-section.

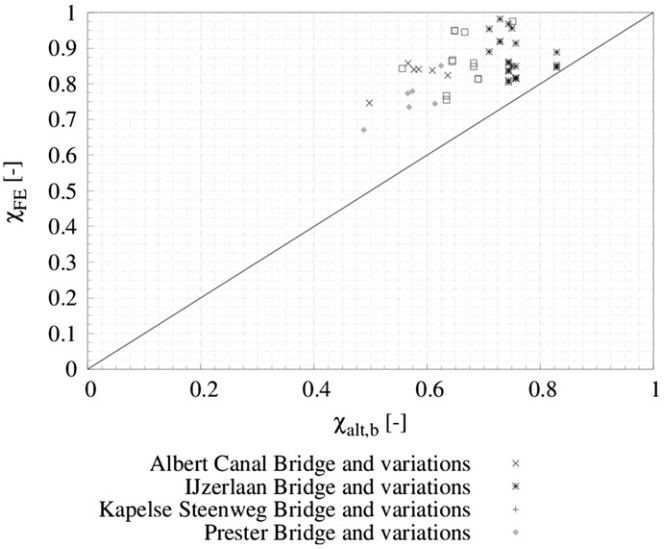

Fig. 16. Comparison of buckling reduction factor as determined by the alternative formula for the buckling length factor and buckling curve "b" and from finite element modelling.

of this analytically determined alternative buckling reduction factor with the one based on detailed finite element modelling is shown in Fig. 16. All of the data points are situated well above the bisector line, indicating that the proposed calculation method still errs on the safe side. The proposed method using β_{alt} apparently never overestimates the buckling capacity of the considered arch bridges.

The results in Fig. 16 are still strictly based on the use of buckling curve "b" for arch bridges. The same buckling calculation can be made, once again using the alternative buckling length factor, but assuming that buckling curve "a" is allowable, leading to an alternative buckling reduction factor $\chi_{alt,a}$. This seams a reasonable assumption since Method I and Fig. 11 already indicated that the present design norms are too conservative. The comparison of the buckling reduction factor $\chi_{alt,a}$ with χ_{FE} is shown in Fig. 17. Comparing both Figs. 16 and 17, it is clear that all of the data points are situated much closer to the bisector line when using buckling curve "a". Still, all of the data points remain above the bisector line indicating that the buckling resistance is never overestimated, even when using buckling curve "a", if the alternative version of the buckling length factor is used.

6. Conclusion

An elaborate and detailed finite element model of a steel tied-arch bridge is used to calculate a large number of geometric variations of six variants of tied-arch bridges with bridge lengths between 50 and 200 m and light wind bracings. Variations include the size of the arch box section, type of bearing system, load type, hanger configuration and amplitude and size of the assumed imperfections. The results of these calculations are then used to determine the resulting relative slenderness and buckling reduction factor. When comparing these values with those determined using Eurocode 3 [2], the results seem quite favourable. While Eurocode 3 dictates the use of buckling curve "b" for the design of arch bridges, all calculation results are situated well above buckling curve "a". Finally, two possible design methods are presented, which will result in a less conservative design. For the first method, the elastic buckling force is determined using a simple finite element model of a perfect arch bridge. The reduction factor can then be determined using buckling curve "a". The second method follows the guidelines of Annex D of Eurocode 3 [2], but proposes an alternative

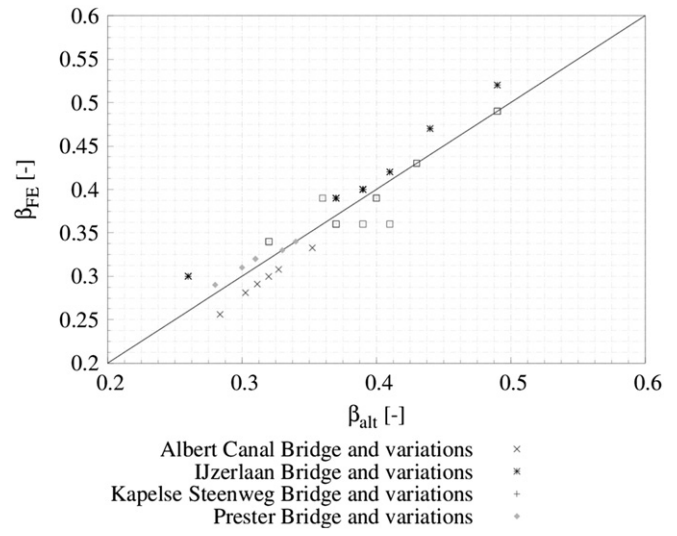

Fig. 15. Comparison of buckling length factors as determined by the alternative formula and from finite element modeling.

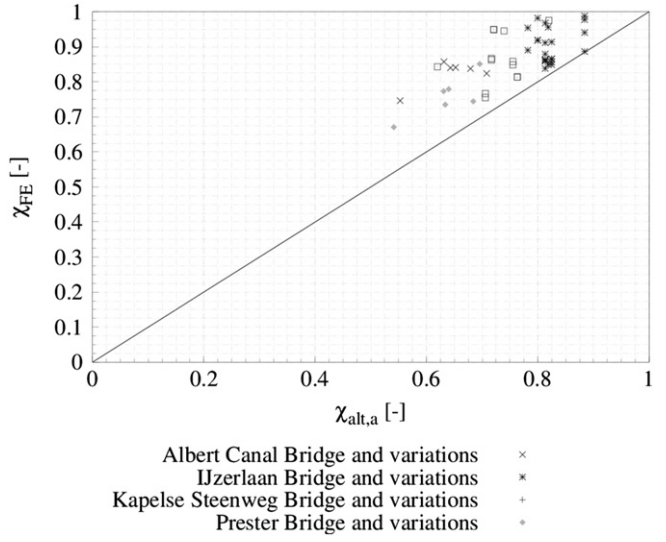

Fig. 17. Comparison of buckling reduction factor as determined by the alternative formula for the buckling length factor and buckling curve "a" and from finite element modelling.

value for the buckling length factor, based on the out-of-plane bending stiffness of the arch.

Eurocode design codes [1,2] are proven to be quite conservative, but if used with an adapted buckling length factor, can allow for using buckling curve "a" for the design of arch bridges. Although the calculation method using an alternative formula for the buckling length factor seems to be pretty straightforward and easy, the advantages of using finite element modelling for buckling design cannot be underestimated since they will always lead to a more accurate design. After all, even the simplified finite element models allow for taking into account the influence of the exact geometry of the arch section, the bending stiffness of the cross-section, the hangers and wind bracings, etc. Although all of these factors have a limited influence on the buckling behaviour when considered separately, together they can have an important impact.

Summarizing it seems that the buckling design of steel tied-arch bridges can be done using strictly analytical formula, as was described in design Method II. However, since a lot of important design parameters are glossed over, this only seems advisable for predesign. For actual design situations, a simplified finite element model such as described in Method I will prove to be a finer design tool for determining the critical buckling load N_{cr}, with only limited additional effort. More detailed finite element modelling such as described in Section 3 seems only interesting for design purposes. Still, for both methods, the use of buckling curve "a" should be considered.

Finally, it is important to underline that all of the discussed results are only assumed to be valid for short and medium span steel tied-arch bridges (50–200 m), not relying on heavy wind bracings. It has to be stressed that this research is only a first indication that a less conservative buckling curve should be considered. Before accepting such a premise, a more extensive and varied set of calculations is necessary as well as prototype testing as validation.

References

[1] Eurocode 3: design of steel structures — part 1–1: general rules and rules for buildings. Brussels: European Committee for Standardization CEN; 2005.
[2] Eurocode 3: design of steel structures — part 2: steel bridges. Brussels: European Committee for Standardization CEN; 2006.
[3] European Convention for Constructional Steelwork. Manual on the stability of steel structures. Paris: Puteaux; 1977.
[4] Pi YL, Trahair NS. Out-of-plane inelastic buckling and strength of steel arches. J Struct Eng 1998;124:174–83.
[5] Spoorenberg RC, Snijder HH, Hoenderkamp JCD, Beg D. Design rules for out-of-plane stability of roller bent steel arches with FEM. J Constr Steel Res 2012;79:9–21.
[6] Bradford MA, Pi YL. A new analytical solution for torsional buckling of arches under axial uniform compression. Eng Struct 2012;41:14–23.
[7] Manzanares Japón JL, Sánchez-Barbudo IH. Non-linear plastic analysis of steel arches under lateral buckling. J Constr Steel Res 2011;67:1850–63.
[8] Heidarpour A, Bradford MA, Othman KAM. Thermoelastic flexural–torsional buckling of steel arches. J Constr Steel Res 2011;67:1806–20.
[9] Pi YL, Bradford MA. Effects of nonlinearity and temperature field on in-plane behavior and buckling of crown-pinned steel arches. Eng Struct 2014;74:1–12.
[10] De Backer H, Outtier A, De Pauw B, Van Bogaert Ph. Long-term monitoring of temperatures in steel box girders. 34th International Symposium on Bridge and Structural Engineering (IABSE — 2010), Venice, Italy; 2010. p. 1–8.
[11] Outtier A, De Backer H, Van Bogaert Ph. Lateral buckling of a steel tied-arch bridge. 10th East Asia Pacific Conference on Structural Engineering & Construction, Bangkok, Thailand: Real Structures and Tall Buildings; 2006. p. 275–80.
[12] Outtier A. A study of the instabilities of arch bridges, based on the determination of geometrical imperfections using strain measurements (in Dutch). [PhD Thesis] Belgium: Ghent University; 2006.
[13] Van Bogaert Ph, Outtier A. Strain measurements as a tool for stability verification of steel tied-arches. In: Radic J, Secon J, editors. Proceedings International Conference on Bridges; 2006. p. 1043–50 Dubrovnik: SECON/CSSE.
[14] LMS SAMTECH - SIEMENS. SAMCEF solver suite. http://www.plm.automation.siemens.com/en_us/products/lms/samtech/samcef-solver-suite/index.shtml; 2014. [Aug. 14, 2014].
[15] Outtier A, De Backer H, De Pauw B, Van Bogaert Ph. Measuring geometrical out-of-plane imperfections in steel tied-arch bridges. Proceedings 5th International Conference on Structural Health Monitoring of Intelligent Infrastructure (SHMII-5 — 2011). Cancun: SHMII; 2011.